Observational Evidence for Reduction of Daily Maximum Temperature by Croplands in the Midwest United States

GORDON B. BONAN

National Center for Atmospheric Research, Boulder, Colorado*

(Manuscript received 7 December 1999, in final form 29 September 2000)

ABSTRACT

Climate model simulations have shown that conversion of natural forest vegetation to croplands in the United States cooled climate. The cooling was greater for daily maximum temperature than for daily minimum temperature, resulting in a reduced diurnal temperature range. This paper presents analyses of observed daily maximum and minimum temperatures that are consistent with the climate simulations. Daily maximum temperature in the croplands of the Midwest United States is reduced relative to forested land in the Northeast, resulting in a decreased diurnal temperature range. The cooling is regional rather than local and is likely created by the contrast between extensive cropland in the Midwest and forest in the Northeast. Seasonal patterns of this cooling are correlated with seasonal changes in crop growth. Analyses of historical temperatures since 1900 and reconstructed cropland extent show a temporal correlation between land use and cooling. The cooling created by the forest–cropland contrast is much more prominent now, when much of the Northeast farmland has been abandoned and reforested, than in the early 1900s when farmlands were more extensive in the Northeast. These results show that human uses of land, especially clearing of forest for agriculture and reforestation of abandoned farmland, are an important cause of regional climate change. Analyses of historical temperature records must consider this ''land use'' forcing.

1. Introduction

The causes of climate change are often ascribed to particular climate forcings such as greenhouse gases, sulfate aerosols, solar irradiance, and volcanic aerosols (Jones et al. 1996; Mann et al. 1998; Hansen et al. 1998, 1999; Tett et al. 1999). Changes in solar irradiance and volcanic eruptions create natural climate system variability while human influences on climate are considered in terms of emissions of greenhouse gases and sulfate aerosols. However, people can also alter climate by clearing land for agriculture. In particular, it is well known that clearing of tropical land for agriculture alters climate (Gash et al. 1996). Climate model studies of the global ''land use'' forcing arising from deforestation and agriculture find it to be significant and comparable to other forcings (Hansen et al. 1998; Brovkin et al. 1999; Chase et al. 2000).

One example of human-mediated landscape change and its effect on climate is in the United States, where the modern vegetated landscape little resembles the natural landscape (Fig. 1). In this figure, modern vegetation is from a 1-km land cover dataset for the period April 1992–March 1993 (Loveland et al. 2000; see also U.S. Geological Survey Earth Resources Observation System Data Center online at http://edcwww.cr.usgs.gov/landdaac/glcc/glcc.html). Natural vegetation is from the VEMAP database (Kittel et al. 1995; see also National Center for Atmospheric Research Climate and Global Dynamics Division online at http://goldhill.cgd.ucar.edu/vemap). Much of the Great Plains prairie and the tree-covered Midwest have been converted to cropland. The temporal history of land cover change is provided by Ramankutty and Foley (1999a), who reconstructed cropland area at 0.5° resolution since 1700 (Fig. 2; see also the Center for Sustainability and the Global Environment, Institute for Environmental Studies, University of Wisconsin—Madison online at http://cpep.aos.wisc.edu). In the northeastern United States, cropland area increased steadily with European settlement, reaching a peak of 50% of the region in 1880. Since then cropland area has declined as farmlands were abandoned and the land was reforested. Rapid settlement of land west of the Appalachian Mountains in the mid-1800s caused cropland area in the Midwest United States to increase from 5% of the region in 1850 to 50% by 1880. Cropland area increased to a peak of over 80% in the late

* The National Center for Atmospheric Research is sponsored by the National Science Foundation.

Corresponding author address: Dr. Gordon B. Bonan, National Center for Atmospheric Research, P.O. Box 3000, Boulder, CO 80307-3000.
E-mail: bonan@ucar.edu

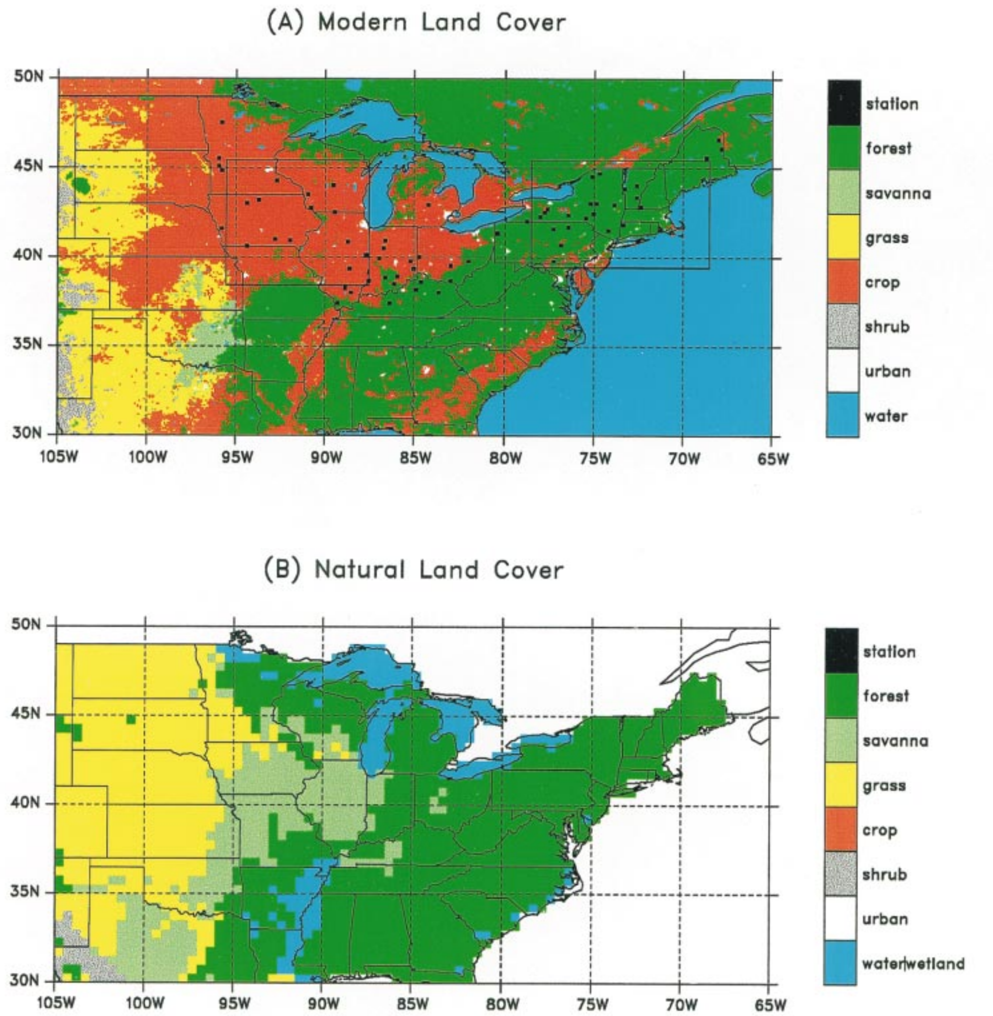

FIG. 1. Modern and natural land cover for the United States east of the Rocky Mountains. (a) The modern land cover has a spatial resolution of 5 min or about 6–8 km. Black squares show the location of the 65 stations used in the study. The classification of these stations into Midwest and Northeast is based on longitude 80.5°W. The two large boxes delineate the Midwest crop (38.5°–45.5°N, 95.5°–87.5°W) and Northeast forest (39.5°–45.5°N, 78.5°–68.5°W) regions used when averaging spatial data. (b) The natural land cover has a spatial resolution of 0.5°.

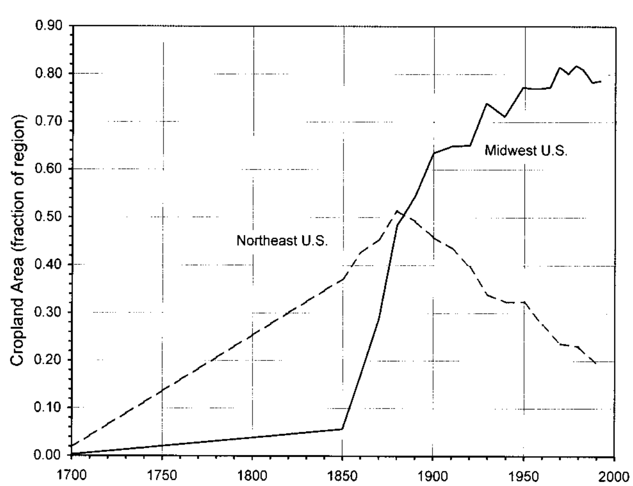

1900s. Williams (1989) presents a thorough review of the history of land clearing in the United States through the 1900s.

Climate simulations with the NCAR Community Climate Model (Kiehl et al. 1998) coupled with the NCAR Land Surface Model (Bonan 1998) show this land clearing cooled climate, primarily in summer and autumn and in the Midwest where daily mean temperature decreased by more than 0.5°C in summer and 2.5°C in autumn (Bonan 1997, 1999). The cooling, which was influenced in the growing season by higher albedo and evapotranspiration in croplands and in au-

←

FIG. 2. Fractional area of croplands in the Northeast and Midwest United States since 1700. The area of the two regions is shown in Fig. 1.

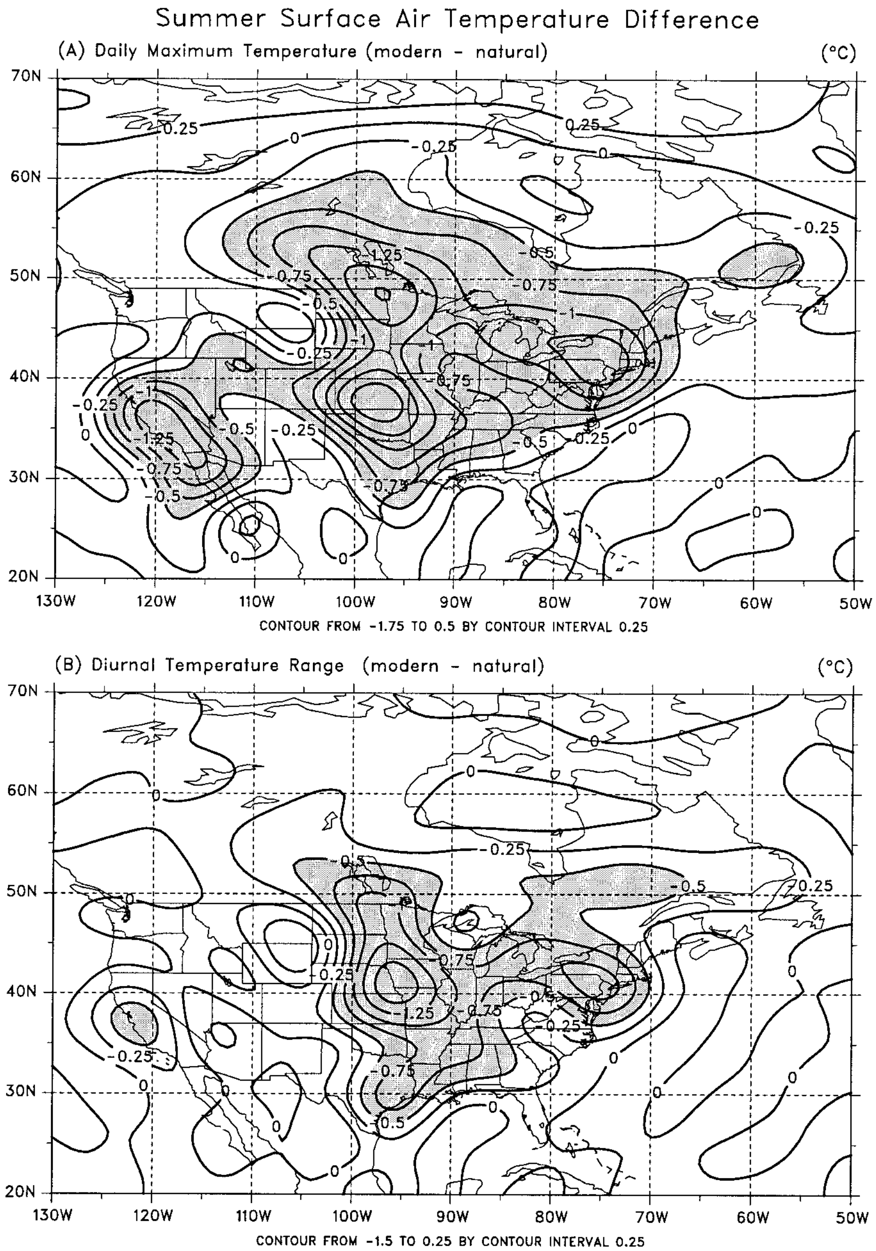

FIG. 3. Difference in summer surface air temperature between 10-yr climate model simulations with modern vegetation and natural vegetation (Bonan 1999). The climate model has a spatial resolution of approximately 2.8° × 2.8° and 18 vertical levels. Climatological sea surface temperatures were used in both simulations, which differed only in land cover (modern or natural). (a) Daily maximum temperature. Regions that cooled by more than 0.5°C are shaded. (b) Diurnal temperature range. Regions where diurnal temperature range decreased by more than 0.5°C are shaded.

tumn from a reduction in leaf area as crops were harvested, was larger during the day than at night, giving a reduced diurnal temperature range of about 1°C (Bonan 1999). Figure 3 shows the reduction in daily maximum temperature and diurnal temperature range for summer. The daytime cooling was largest (1.5°C) in the Midwest where the model had extensive croplands but extended to the northeastern United States where the model had partial deforestation. The cooling in California arose from conversion of natural grassland to cropland. Diurnal temperature range decreased by more than 0.5°C throughout the eastern United States with larger decreases in the Midwest (0.75°–1.5°C) than in the East (0.75°–1.0°C). Spring

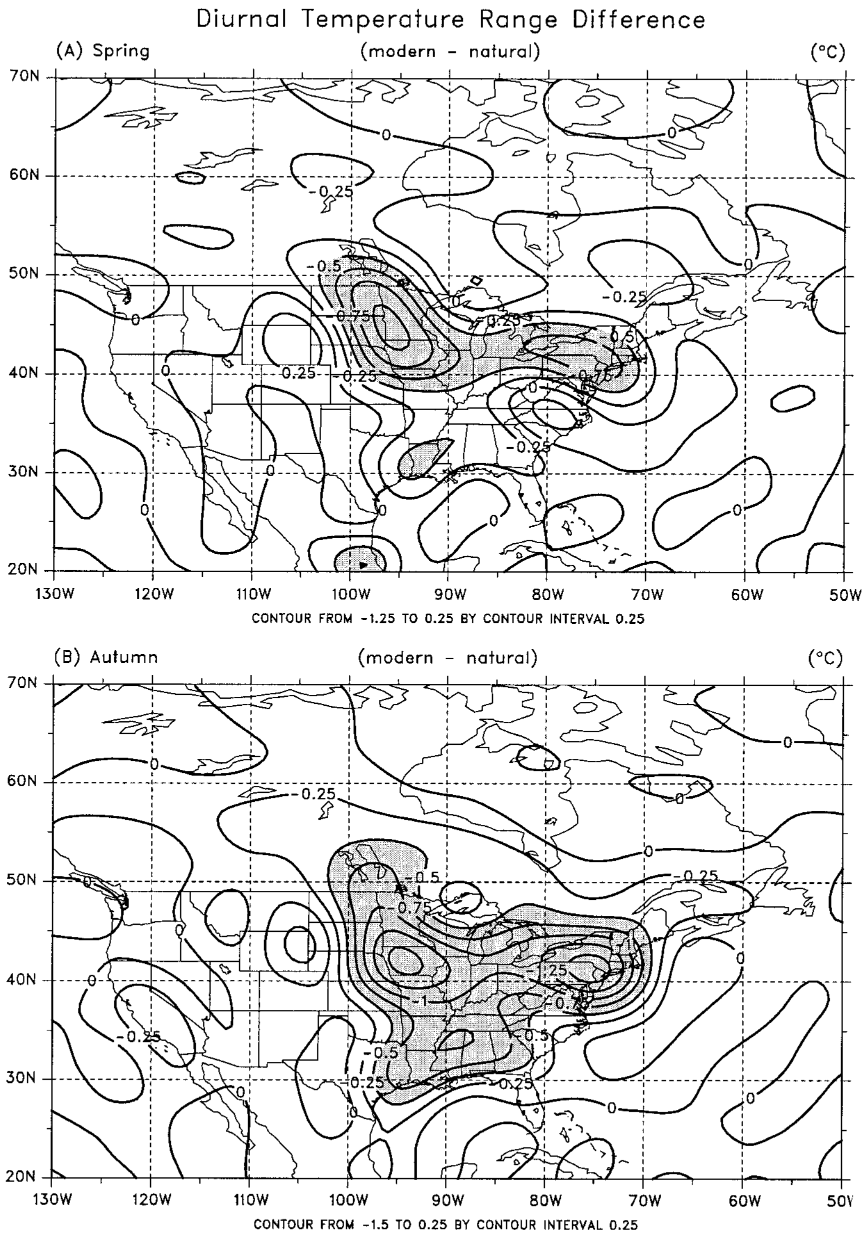

FIG. 4. Difference in diurnal temperature range between 10-yr climate model simulations with modern vegetation and natural vegetation (Bonan 1999). See Fig. 3 for a description of these simulations. Regions where diurnal temperature range decreased by more than 0.5°C are shaded. (a) Spring; (b) autumn.

and autumn had similar decreases in diurnal temperature range; winter showed negligible change (Fig. 4). In spring, the Midwest had a larger decrease in diurnal temperature range (greater than 1°C) than the Northeast (0.5°–1.0°C). In autumn, both regions had similar decreases (greater than 1°C).

Here, I present observational evidence that conversion of tree-covered regions of the Midwest United States to cropland has cooled maximum daily temperature and reduced diurnal temperature range. The preferred method to detect a land use signal is to relate temporal changes in temperature to concomitant changes in land cover. However, high-resolution land cover maps are only available for current or recent land use (e.g., Fig. 1). Past land uses must be reconstructed from historical records (Houghton et al. 1999; Ramankutty and Foley 1999a,b) and may not have sufficient accuracy to detect a land use signal in light of other ongoing climate forcings (e.g., solar variability, volcanic aerosols, greenhouse gases). In-

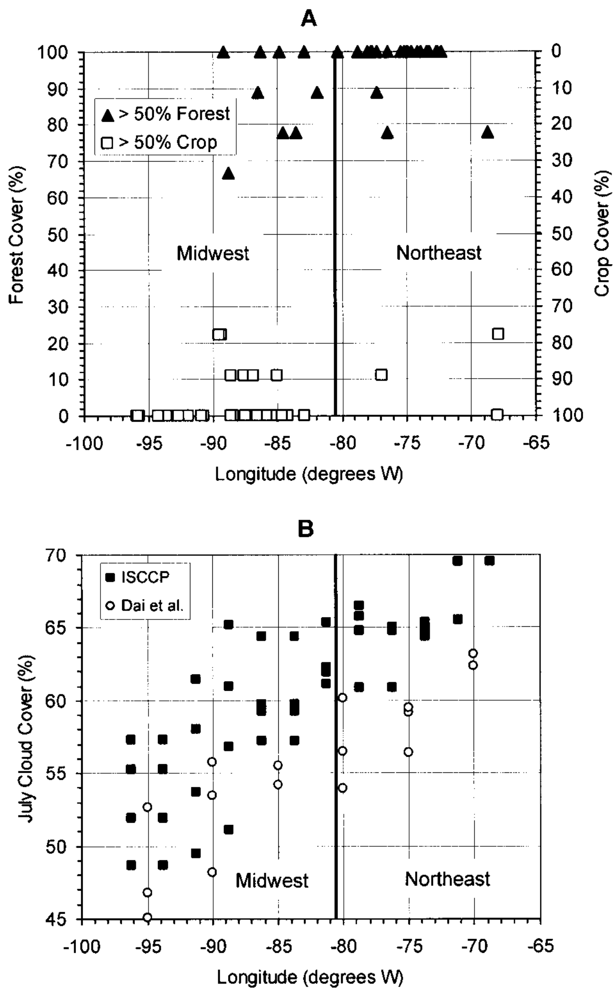

FIG. 5. Longitudinal trends in land use and cloud cover. The thick vertical line at 80.5°W separates the longitudinal gradient into the Midwest and Northeast regions. (a) Forest and crop cover for the 65 stations used in the analyses. For these stations, forest and crop cover sum to 100%. Stations are classified as forest or crop based on a 50% threshold. (b) Jul cloud cover for 42 ISCCP and 17 Dai et al. (1999) land grid cells covering the same geographic region as the station data.

stead, spatial patterns of current maximum and minimum daily temperatures were related to spatial variation in land cover.

2. Methods

Monthly averaged daily maximum and minimum temperature were obtained from the U.S. Historical Climatology Network (U.S. HCN; Easterling et al. 1996; see also the National Climatic Data Center online at http://www.ncdc.noaa.gov/ol/climate/research/ushcn/ushcn.html). Temperatures for these 1221 stations have been adjusted for changes in time of observations, instruments, station locations, and urbanization. Surrounding land cover at 100, 1000, and 10 000-m distances are available for 1219 stations. Previous studies utilizing this ancillary land-cover data have emphasized the effect of urbanization to reduce diurnal temperature range (Gallo et al. 1996, 1999). A monthly climatology of daily maximum temperature (T_{max}), daily minimum temperature (T_{min}), and diurnal temperature range (DTR = $T_{max} - T_{min}$) was created for the 10-yr period 1986–95.

Local and regional differences in land cover among stations might introduce temperature biases that obscure any temperature change related to the presence of croplands. In particular, coastal sites and stations located near large water bodies will be affected by maritime influences. Proximity to water was based on a 1-km land-cover dataset for North America (Fig. 1a). Stations with any water present on a 101 km × 101 km grid centered on the station were excluded from the analyses. In addition, local land cover in the immediate vicinity of the stations (e.g., forest, urban, airport) might create different microclimates. Differences in local land cover were accounted for by selecting only stations that at 100-m distance were classified as ''nonvegetated,'' ''open farmland, grasslands,'' or ''small town less than 1000 population'' in the U.S. HCN land cover dataset. This excluded ''coastal,'' ''forest,'' ''town 1000 to 10 000 population,'' ''city area,'' ''airport,'' and ''unknown'' categories. To further ensure that stations in large metropolitan areas were excluded, the 1-km land cover (Fig. 1a) was used to remove stations with any urban cover on a surrounding 101 km × 101 km grid. With these filters, stations selected for analysis are in rural open locations far from large water bodies.

Each of the selected stations was classified by dominant vegetation cover. The U.S. HCN ancillary land cover does not adequately distinguish vegetation types. While forested lands are distinguished by a forest land cover, croplands and grasslands are mixed into an open farmland, grassland cover type. Instead, the 1-km land cover for North America (Fig. 1a) was used to define seven land cover classes (forest, crop, grass, shrub, barren, water, urban) around each station. Each station was assigned a land cover based on the dominant land cover in a 3 km × 3 km grid centered on the station.

The effect of forest and crops on temperature were analyzed using 65 stations in a 17-state area of the Northeast and Midwest United States (Fig. 1). In these areas, the natural land cover was predominantly forest or savanna and the modern land cover is forest or cropland. The average elevation of stations does not differ greatly between the two regions (Northeast: 241 m; Midwest: 253 m). However, geographic differences in land cover among the stations preclude stratification of the data by climatic divisions. Forest cover increases with eastward longitudes [Fig. 5a, $r = 0.671$, $p < 0.001$ (the convention in this study is that longitudes increase from west to east)]. The Midwest stations are predominantly cropland (30 of 39 sta-

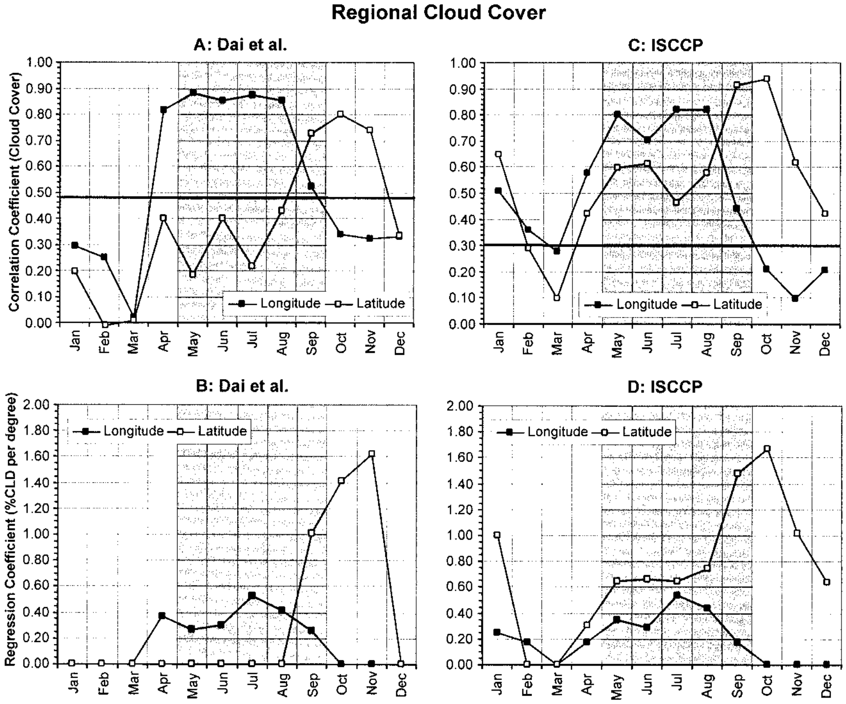

FIG. 6. Monthly relationships among cloud cover, latitude, and longitude for the Midwest and northeastern United States. Both the Dai et al. (1999) station data (a), (b) and the ISCCP satellite data (c), (d) are shown. Shaded months show the 5-month crop growing season. (a) Correlation of Dai et al. (1999) cloud cover with longitude and latitude for 17 grid cells corresponding to the study area. Correlation coefficients greater than $r = 0.482$ (thick horizontal line) are statistically significant ($p < 0.05$). (b) Slope obtained from linear regression of Dai et al. (1999) cloud cover with longitude and latitude. (c) Correlation of ISCCP cloud cover with longitude and latitude for 42 grid cells corresponding to the study area. Correlation coefficients greater than $r = 0.304$ (thick horizontal line) are statistically significant ($p < 0.05$). (d) Slope obtained from linear regression of ISCCP cloud cover with longitude and latitude.

tions); Northeast stations are predominantly forested (23 of 26 stations).

Hence, temperature differences between cropland (Midwest) and forest (Northeast) stations are affected by factors in addition to land use. In particular, cloud cover dampens DTR by reducing T_{max} (Dai et al. 1997, 1999). Two cloud cover datasets were used to examine regional differences in cloud cover: climatological cloud cover from the International Satellite Cloud Climatology Project (ISCCP) for 1983–91 (Rossow and Garder 1993a,b; Rossow et al. 1993) gridded to a 2.5° resolution (online at http://isccp.giss.nasa.gov); and a 4° lat × 5° long climatological dataset for 1980–91 derived from station observations and used by Dai et al. (1999) in their analysis of the effects of clouds on DTR (A. Dai 2000, personal communication). Based on the 42 ISCCP land grid cells covering the same geographic region as the station data (38.75°–46.25°N, 96.25°–68.75°W), there are indeed strong regional differences in cloud cover. For example, July cloud cover increases with eastward longitudes (Fig. 5b, $r = 0.820$, $p < 0.001$). The Dai et al. (1999) station data (using 17 grid cells) show the same geographic trend (Fig. 5b, $r = 0.875$, $p < 0.001$), though the two datasets differ in cloud amount. Throughout the year, monthly cloud cover in the study region generally increases to the east, with strong northward increases in autumn (Figs. 6, 7, and 8). Both datasets show cloud cover is highly positively correlated with eastward longitudes during April–August, increasing at a rate of 1.7% to 5.4% (10° long)$^{-1}$ (ISCCP) and 2.7% to 5.2% (10° long)$^{-1}$ (Dai et al. 1999), and to a lesser extent in September (Fig. 6). The datasets differ primarily in the relationship of cloud cover with latitude in spring and summer, perhaps because of the sparse (3 or 4 grid cells) latitudinal range (Fig. 5b).

Dai et al. (1999) showed that mean monthly DTR decreases with increased monthly cloud cover as a result of reduced daytime surface heating. While one can not discount possible geographic differences in the diurnal cycle of clouds (and the effect of this on DTR), the study of Dai et al. (1999) suggests stations in the Midwest, with less cloud cover, should have a larger DTR in comparison with stations in the Northeast. Geographic differences in precipitation also affect T_{max} by sustaining higher rates of evapotranspi-

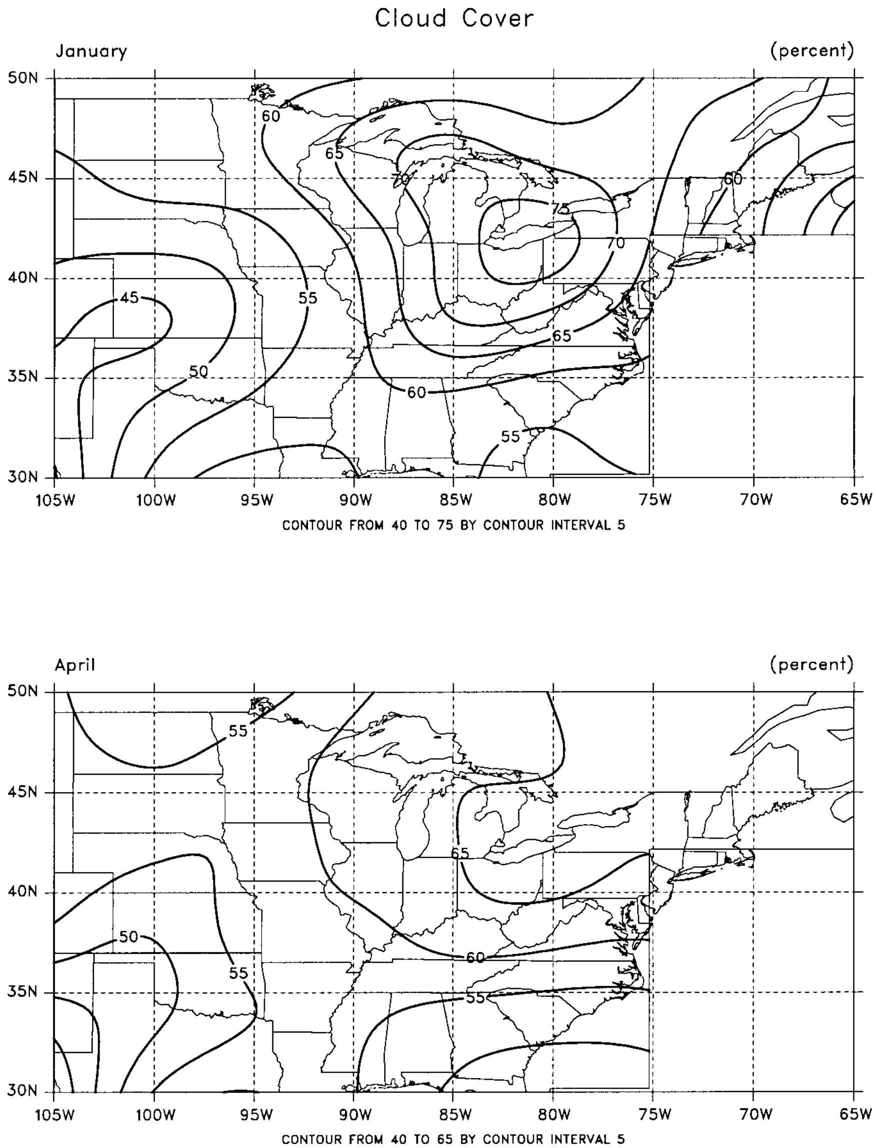

FIG. 7. Dai et al. (1999) cloud cover for Jan and Apr.

ration, but clouds have the dominant effect (Dai et al. 1999).

3. Results and discussion

a. Longitudinal trends in monthly T_{max}, T_{min}, and DTR

Simple linear correlation between station DTR and longitude showed DTR increases with eastward longitudes from February to July except April (Fig. 9a). DTR decreases with eastward longitudes only in April, September, and October. The May, June, and July positive correlations between station DTR and longitude and the August lack of correlation are particularly significant because these are months with strong eastward increase in cloud cover (Fig. 6). The lack of decrease in DTR with eastward longitudes is opposite of what is expected from increased cloud cover. Greater cloud cover in the east should reduce DTR compared to western stations (Dai et al. 1999).

Further insight to the causes of the eastward increase in DTR was provided by a multiple regression model that related monthly station T_{max} and T_{min} to station latitude, longitude, and elevation. These regression models accounted for 91%–98% of the variation in T_{max} and 85%–97% of the variation in T_{min} (except October when $r^2 = 0.74$). They showed seasonally varying decrease in temperature with northern latitudes (Fig. 9b), with greatest latitudinal cooling in winter, and 0.2°–0.8°C cooling per 100-m increase in elevation (Fig. 9c). The longitudinal gradient in T_{max} and T_{min} is near zero or positive from October to Feb-

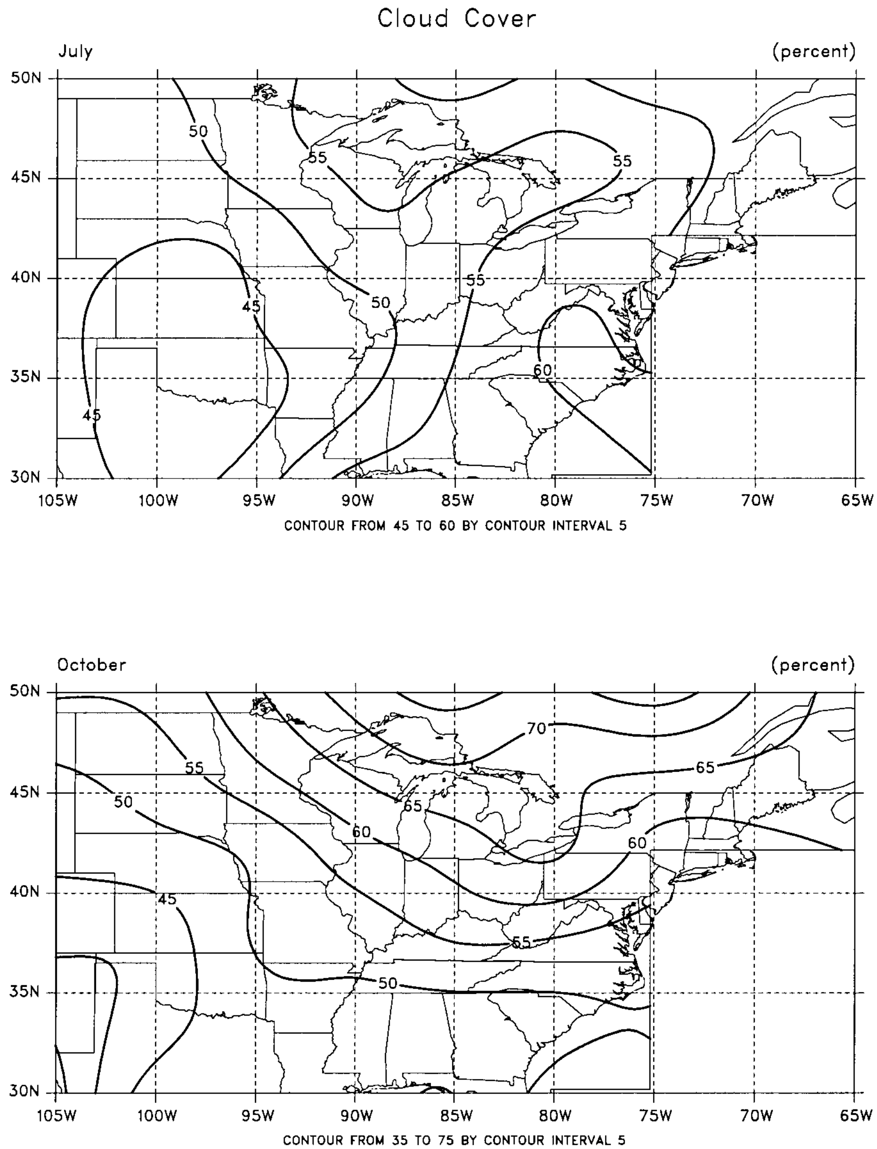

FIG. 8. Dai et al. (1999) cloud cover for Jul and Oct.

ruary, when cloud cover has a weak longitudinal dependence, and negative for the remainder of the year as expected from the increase in cloud cover (Fig. 9d).

The regression equations showed that in the months when DTR increases with eastward longitudes (February, March, May, June, and July), it does so because the longitudinal rate at which T_{max} cools is significantly less than that of T_{min} (Fig. 9d). This is opposite of what is expected from the greater cloud cover for eastern stations in comparison with western stations (Fig. 10). If cloud cover affected T_{max} and T_{min} similarly, one would expect equal rates of eastward cooling so that DTR does not change with longitude. In fact, cloud cover depresses T_{max} more than T_{min} (Dai et al. 1999) so that the longitudinal cooling of T_{max} should exceed that of T_{min} and DTR decreases with eastward sites. The observations, however, show the opposite. The T_{max} cools at a lesser rate than T_{min} so that DTR increases with eastward longitudes.

The eastward increase in DTR as a result of smaller eastward cooling of T_{max} is consistent with climate model simulations showing croplands cool temperatures in comparison with forest and that this cooling is greatest for T_{max} (Bonan 1999). The extensive croplands in the Midwest reduce T_{max} as compared with forested regions to the east so that the longitudinal gradient is dampened relative to that of T_{min}. Moreover, the observed seasonality of the eastward increase in DTR is consistent with the climate model simulations. The observations show this eastward increase is statistically significant in two of three spring

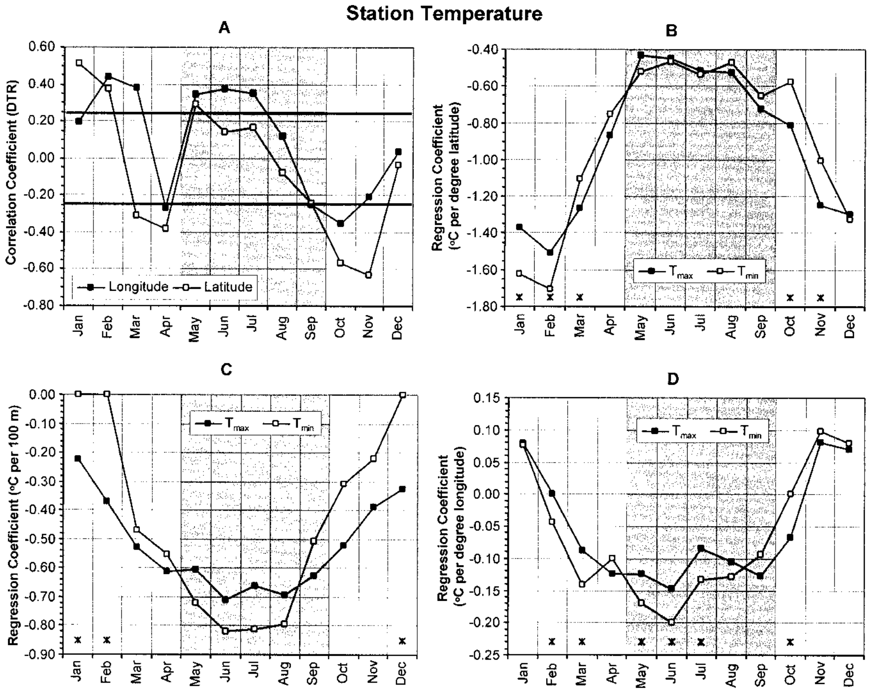

FIG. 9. Monthly relationships among station temperature, latitude, longitude, and elevation for the Midwest and northeastern United States. Shaded months show the 5-month crop growing season. (a) Correlation of DTR with latitude and longitude for the 65 stations. Correlation coefficients above or below the thick horizontal lines ($r = \pm 0.244$) are statistically significant ($p < 0.05$). (b) Latitudinal gradient for T_{max} and T_{min} from multiple-regression models relating station temperature to latitude, elevation, and longitude. (c) Elevation gradient for T_{max} and T_{min} from the regression models. (d) Longitudinal gradient for T_{max} and T_{min} from the regression models. For (b), (c), and (d), * denotes coefficients that are statistically different between T_{max} and T_{min} ($p < 0.05$).

months (March, May), in two of three summer months (June, July), but not in autumn (Figs. 9a, d). The climate model simulations showed conversion of tree-covered land to cropland caused a greater reduction in DTR in the Midwest than in the Northeast in spring (Fig. 4a) and summer (Fig. 3b) but that the autumn reduction occurred equally in both regions (Fig. 4b).

Because the longitudinal trend in T_{max} is influenced by both clouds and croplands, it is difficult to quantify the cooling influence of croplands. The cooling rate of T_{min} represents the null model of no geographic influence from clouds, and the difference in cooling rates between T_{max} and T_{min} indicates the minimum cooling influence (Fig. 10). In May, June, and July, this difference ranges from 0.045° to 0.052°C (° long)$^{-1}$. The forest and crop regions outlined in Fig. 1 are separated on average by 18° longitude, implying the cropland region is at least 0.8°–0.9°C cooler than expected. Because decreased cloud cover in the Midwest warms T_{max} relative to T_{min}, the actual cooling from croplands is even greater.

This cooling appears to be a manifestation of regional rather than local land use. Analyses for all stations except those near large water bodies (252 stations) were similar to those for the 65 rural open stations. This likely reflects the broad, spatially cohesive patterns of land use in which the Midwest is almost exclusively cropland while the Northeast is predominantly forested (Fig. 1).

b. Relation to vegetation phenology

The period from May to September is particularly noteworthy. Surface albedo obtained from the Earth Radiation Budget Experiment satellite measurements for 1985–89 gridded to 2.5° resolution (Li and Garand 1994) is relatively constant, at seasonally low values, and croplands have a higher albedo (by 0.03–0.04) than forests (Figs. 11a,b; see also the Canadian Centre for Remote Sensing online at http://www.ccrs.nrcan.gc.ca). The cropland area is dominated by corn, soybeans, and oats with some wheat and hay pastures (see also the U.S. Department of Agriculture Natural Resources Conservation Service online at http://www.nhq.nrcs.usda.gov/land/home.html). Corn is typically sown during April and May while soybeans are sown in May and June. These crops reach silking (corn) and flowering (soybean) stages in July, mature in August, and are harvested in September and October.

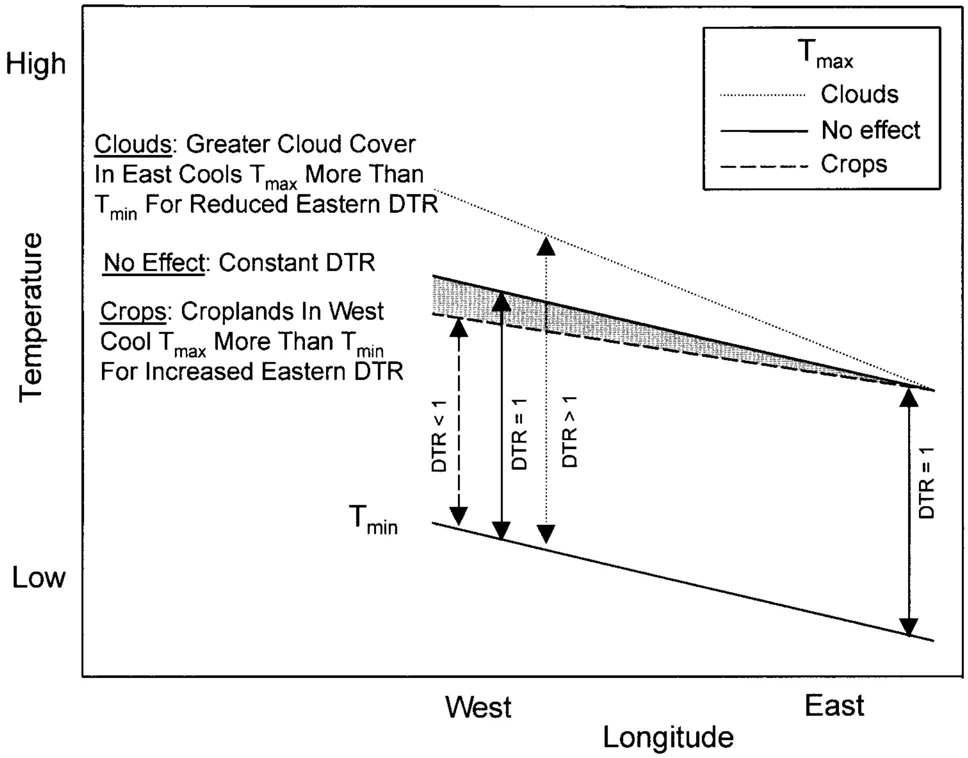

FIG. 10. Observed west–east trends in T_{max} relative to T_{min} in comparison with expected trends assuming a constant DTR and a reduction in DTR due to clouds. The vertical arrows show the magnitude of DTR relative to no longitudinal change in DTR. The cooling rate of T_{min} represents the null model of no geographic influence from clouds or croplands. The shaded region represents the minimal cooling associated with croplands in the Midwest.

This pheneological development is seen in photosynthetic activity as measured by the 14-yr (July 1981–September 1994) Pathfinder advanced very high resolution radiometer monthly composite normalized difference vegetation index (NDVI; Tucker et al. 1985, 1986; Myneni et al. 1997; Braswell et al. 1997) gridded to 1° resolution (Figure 11a; see also National Aeronautics and Space Administration Goddard Space Flight Center online at http://daac.gsfc.nasa.gov). For the Midwest crop and Northeast forest areas, the greatest monthly ''greening up,'' as measured by the monthly difference in NDVI, occurs between April and May as both the trees and crops begin to grow. The forest region has a higher NDVI than cropland. The difference in NDVI between the crop and forest regions increases early in the growing season, reaching maximum values in May and June when the crops are sown or immature but the trees are readily photosynthesizing (Fig. 11b). The NDVI difference is smallest in July and August when the crops are most productive and increases again in autumn as crops are harvested. During this period cloud cover increases to the east (Fig. 6), but DTR decreases with eastward longitudes in only one of five months because for four months T_{max} cools at a rate less than or equal to that of T_{min} (Figs. 9a,d). DTR decreases with eastward longitudes, as expected from increased cloud cover, only in September.

The 5-month growing season is a period of seasonally high rates of temperature cooling with respect to elevation (Fig. 9c), seasonally low decreases in temperature with northern latitudes (Fig. 9b), and seasonally high rates of temperature cooling with eastward longitudes (Fig. 9d). This study cannot determine if the temporal relationship between crop growth and DTR is causal or merely a correlation between independent, seasonally varying variables. However, it is plausible that crop physiological activity determines the difference in longitudinal gradients between T_{max} and T_{min} and hence DTR. The higher albedo of croplands in comparison with forests cools temperature by reflecting more solar radiation and was identified as one of the causal factors in the simulated cooling from deforestation (Bonan 1997, 1999). In the climate model simulations, the autumn harvesting of crops caused the cooling to decrease (Bonan 1999), which may explain the decreased DTR longitudinal gradient seen in both the model and observations in autumn in comparison with spring and summer.

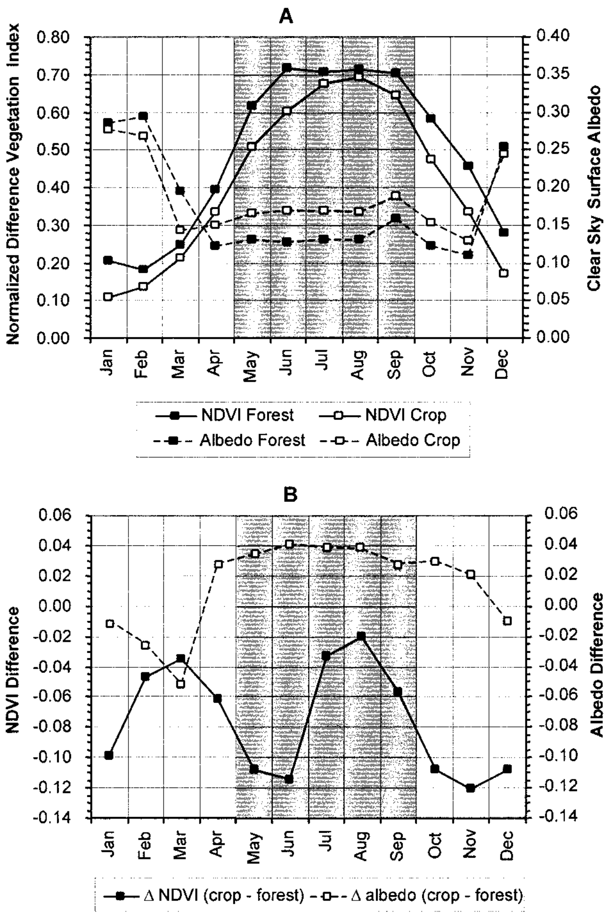

FIG. 11. Satellite-derived vegetation phenology. (a) Monthly NDVI and surface albedo for the Northeast forest and the Midwest crop regions. Fig. 1 shows the forest and crop regions (land only) over which NDVI and albedo were averaged. (b) Difference in NDVI and albedo between the crop and forest regions.

c. Historical changes in T_{max}, T_{min}, and land cover

Regression equations that related station T_{max} and T_{min}, averaged for the 4-month period May–August, to latitude, longitude, and elevation were developed using U.S. HCN temperatures for each year from 1900 to 1995. Over this 96-yr period, the regression equations accounted for 69%–96% of the variation in T_{max} and 74%–92% of the variation in T_{min}. For both temperatures, 80% of the years had $r^2 > 0.80$.

The regression coefficients relating T_{max} and T_{min} to longitude varied considerably over the 96-yr period (Figs. 12a,b). In each year the coefficients are negative, meaning temperatures cool with eastward longitudes as expected from the greater cloud cover in the east. The regression coefficient for T_{min} does not show a prominent temporal trend, but the coefficient for T_{max} becomes less negative (i.e., the longitudinal cooling is weaker) from 1988 to 1993—a time period that is encompassed by this study, which uses average temperatures for 1986–95. The difference between the regression coefficients

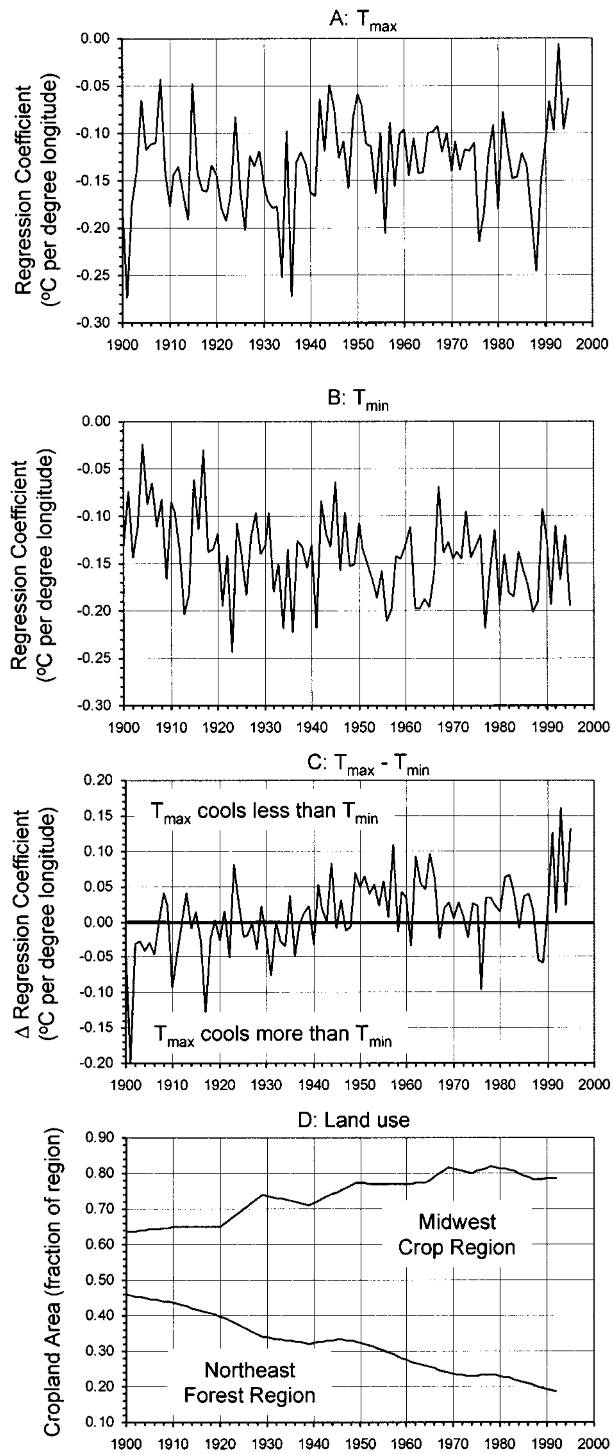

FIG. 12. Temporal changes in temperature and land cover since 1900. (a) Longitudinal gradient for T_{max} averaged for 4-month period May–Aug. (b) Longitudinal gradient for T_{min} averaged for 4-month period May–Aug. (c) Difference in regression coefficients. (d) Cropland area in the Midwest and Northeast regions.

for T_{max} and T_{min} also varies considerably from year to year (Fig. 12c). A positive difference means the coefficient for T_{max} is less negative than that of T_{min}, indicating weaker longitudinal cooling; a negative difference means T_{max} cools with eastward longitudes at a greater rate than T_{min}. The 10-yr study period has the three largest positive differences (1991, 1993, 1995) during the 96-yr record.

Is the 10-yr study period unique or do other periods show similar results? Over the 96-yr record, the longitudinal cooling of T_{max} is less than that of T_{min} in 57 yr. However, the difference in regression coefficients between T_{max} and T_{min} tends to become more positive over time, indicating weaker longitudinal cooling for T_{max} over time. Prior to 1940, this difference tends to be negative; it is positive for only 14 of 40 yr (35%). Since 1940, it is positive for 43 of 56 yr (77%).

The positive difference since 1940 coincides with the time period over which DTR has decreased in the United States and globally (Karl et al. 1993; Easterling et al. 1997). This is a result of differential changes in T_{max} and T_{min} in which T_{min} warms at a faster rate or cools at a slower rate than T_{max}. It is largely related to increased cloud cover over time. It is possible that the differences in eastward temperature cooling for T_{max} and T_{min} found in this study reflect geographic variation in this trend and not land use. For example, if over time DTR decreased more or increased less in the Midwest than in the Northeast, then one could conceivably find a smaller DTR in the Midwest than in the Northeast. In the United States, DTR has increased in spring and decreased in summer and autumn in both the Northeast and Midwest (Plantico et al. 1990; Karl et al. 1984, 1986). However, the springtime increase in DTR is greater in the Midwest than in the Northeast. The summer and autumn decreased DTR is caused by cooling of T_{max} and weak warming in T_{min}. The decrease in T_{max} is greater for the Northeast than for the Midwest in both seasons. It is unlikely, therefore, that the results found in this study reflect merely temporal changes in DTR related to increased cloud cover.

Could the observed temporal changes in DTR reflect changes in land use? Figure 12d shows temporal changes in cropland area for the Midwest and Northeast between 1900 and 1992 as reconstructed by Ramankutty and Foley (1999a). During this time, cropland area in the Northeast decreased from 46% of the land to 19% while cropland area in the Midwest increased from 64% to 79% of the land. As the Northeast cropland was abandoned and reforested, one would expect warming of T_{max} and hence an increase in DTR. Since the observations show the opposite, it is unlikely that land use has contributed to the observed decrease in DTR.

However, the data in Fig. 12 show a temporal correlation between land use and temperature. Abandonment of farms in the Northeast and expansion of farms in the Midwest created a greater land use contrast between the two regions throughout the 1900s. In 1900, the difference in cropland extent was relatively minor (64% in the Midwest, 46% in the Northeast). By 1992, farms comprised 79% of the Midwest but only 19% of the Northeast (Fig. 12d). The long-term trend of farm abandonment and reforestation in the Northeast is consistent with temporal trends in the eastward increase in DTR found in this study. The current eastward increase in DTR is created by the contrast in extensive cropland in the Midwest and forest in the Northeast. In the early 1900s, when both regions were heavily farmed, the eastward increase in DTR was not as prominent as today, when much of the farmland in the Northeast has been abandoned and reforested.

4. Conclusions

Human land uses such as deforestation, grazing, crops, and urbanization are becoming recognized as important climate forcings at local to regional scales (Couzin 1999). Observations show a variety of land uses such as urban development (Landsberg 1981), tropical deforestation (Gash et al. 1996), and overgrazing of arid lands (Balling 1988, 1989; Balling et al. 1998) warm local and regional climate. Irrigation in the dry plains of Colorado may cool climate (Stohlgren et al. 1998; Chase et al. 1999). As this study shows, clearing of temperate forests for agriculture in the Midwest and Northeast regions of the United States likely cooled climate while subsequent reforestation of abandoned farms in the Northeast warmed climate. These land uses must be added to the growing list of land use impacts on climate.

Acknowledgments. I thank Aiguo Dai for numerous helpful comments on this manuscript and for providing his station cloud data.

REFERENCES

Balling, R. C., Jr., 1988: The climatic impact of a Sonoran vegetation discontinuity. *Climatic Change,* **13,** 99–109.

——, 1989: The impact of summer rainfall on the temperature gradient along the United States–Mexico border. *J. Appl. Meteor.,* **28,** 304–308.

——, J. M. Klopatek, M. L. Hildebrandt, C. K. Moritz, and C. J. Watts, 1998: Impacts of land degradation on historical temperature records from the Sonoran Desert. *Climatic Change,* **40,** 669–681.

Bonan, G. B., 1997: Effects of land use on the climate of the United States. *Climatic Change,* **37,** 449–486.

——, 1998: The land surface climatology of the NCAR land surface model coupled to the NCAR Community Climate Model. *J. Climate,* **11,** 1307–1326.

——, 1999: Frost followed the plow: Impacts of deforestation on the climate of the United States. *Ecol. Appl.,* **9,** 1305–1315.

Braswell, B. H., D. S. Schimel, E. Linder, and B. Moore III, 1997: The response of global terrestrial ecosystems to interannual temperature variability. *Science,* **278,** 870–872.

Brovkin, V., A. Ganopolski, M. Claussen, C. Kubatzki, and V. Petoukhov, 1999: Modelling climate response to historical land cover change. *Global Ecol. Biogeogr.,* **8,** 509–517.

Chase, T. N., R. A. Pielke Sr., T. G. F. Kittel, J. S. Barron, and T. J.

Stohlgren, 1999: Potential impacts on Colorado Rocky Mountain weather due to land use changes on the adjacent Great Plains. *J. Geophys. Res.,* **104,** 16 673–16 690.

——, ——, ——, R. R. Nemani, and S. W. Running, 2000: Simulated impacts of historical land cover changes on global climate in northern winter. *Climate Dyn.,* **16,** 93–105.

Couzin, J., 1999: Landscape changes make regional climate run hot and cold. *Science,* **283,** 317–319.

Dai, A., A. D. Del Genio, and I. Y. Fung, 1997: Clouds, precipitation, and temperature range. *Nature,* **386,** 665–666.

——, K. E. Trenberth, and T. R. Karl, 1999: Effects of clouds, soil moisture, precipitation, and water vapor on diurnal temperature range. *J. Climate,* **12,** 2451–2473.

Easterling, D. R., T. R. Karl, E. H. Mason, P. Y. Hughes, and D. P. Bowman, 1996: United States Historical Climatology Network (U.S. HCN) monthly temperature and precipitation data. Oak Ridge National Laboratory ORNL/CDIAC-87, NDP-019/R3, Carbon Dioxide Information Analysis Center, 280 pp. [Available from National Technical Information Service, 5285 Port Royal Rd., Springfield, VA 22161.]

——, and Coauthors, 1997: Maximum and minimum temperature trends for the globe. *Science,* **277,** 364–367.

Gallo, K. P., D. R. Easterling, and T. C. Peterson, 1996: The influence of land use/land cover on climatological values of the diurnal temperature range. *J. Climate,* **9,** 2941–2944.

——, T. W. Owen, D. R. Easterling, and P. F. Jamason, 1999: Temperature trends of the U.S. Historical Climatology Network based on satellite-designated land use/land cover. *J. Climate,* **12,** 1344–1348.

Gash, J. H. C., C. A. Nobre, J. M. Roberts, and R. L. Victoria, Eds., 1996: *Amazonian Deforestation and Climate.* John Wiley and Sons, 611 pp.

Hansen, J. E., M. Sato, A. Lacis, R. Ruedy, I. Tegen, and E. Matthews, 1998: Climate forcings in the industrial era. *Proc. Natl. Acad. Sci. USA,* **95,** 12 753–12 758.

——, R. Ruedy, J. Glascoe, and M. Sato, 1999: GISS analysis of surface temperature change. *J. Geophys. Res.,* **104,** 30 997–31 022.

Houghton, R. A., J. L. Hackler, and K. T. Lawrence, 1999: The U.S. carbon budget: Contributions from land-use change. *Science,* **285,** 574–578.

Jones, P. D., R. S. Bradley, and J. Jouzel, Eds., 1996: *Climatic Variations and Forcing Mechanisms of the Last 2000 Years.* Springer-Verlag, 649 pp.

Karl, T. R., G. Kukla, and J. Gavin, 1984: Decreasing diurnal temperature range in the United States and Canada from 1941 through 1980. *J. Climate Appl. Meteor.,* **23,** 1489–1504.

——, ——, and ——, 1986: Relationship between decreased temperature range and precipitation trends in the United States and Canada, 1941–80. *J. Climate Appl. Meteor.,* **25,** 1878–1886.

——, and Coauthors, 1993: Asymmetric trends of daily maximum and minimum temperature. *Bull. Amer. Meteor. Soc.,* **74,** 1007–1023.

Kiehl, J. T., J. J. Hack, G. B. Bonan, B. B. Boville, D. L. Williamson, and P. J. Rasch, 1998: The National Center for Atmospheric Research Community Climate Model: CCM3. *J. Climate,* **11,** 1131–1149.

Kittel, T. G. F., N. A. Rosenbloom, T. H. Painter, D. S. Schimel, and VEMAP Modeling Participants, 1995: The VEMAP integrated database for modeling United States ecosystem/vegetation sensitivity to climate change. *J. Biogeogr.,* **22,** 857–862.

Landsberg, H. E., 1981: *The Urban Climate.* Academic Press, 275 pp.

Li, Z., and L. Garand, 1994: Estimation of surface albedo from space: A parameterization for global application. *J. Geophys. Res.,* **99,** 8335–8350.

Loveland, T. R., B. C. Reed, J. F. Brown, D. O. Ohlen, Z. Zhu, L. Yang, and J. W. Merchant, 2000: Development of a global land cover characteristics database and IGBP DISCover from 1 km AVHRR data. *Int. J. Remote Sens.,* **21,** 1303–1330.

Mann, M. E., R. S., Bradley, and M. K. Hughes, 1998: Global-scale temperature patterns and climate forcing over the past six centuries. *Nature,* **392,** 779–787.

Myneni, R. B., C. D. Keeling, C. J. Tucker, G. Asrar, and R. R. Nemani, 1997: Increased plant growth in the northern high latitudes from 1981 to 1991. *Nature,* **386,** 698–702.

Plantico, M. S., T. R. Karl, G. Kukla, and J. Gavin, 1990: Is recent climate change across the United States related to rising levels of anthropogenic greenhouse gases? *J. Geophys. Res.,* **95,** 16 617–16 637.

Ramankutty, N., and J. A. Foley, 1999a: Estimating historical changes in global land cover: Croplands from 1700 to 1992. *Global Biogeochem. Cycles,* **13,** 997–1027.

——, and ——, 1999b: Estimating historical changes in land cover: North American croplands from 1850 to 1992. *Global Ecol. Biogeogr.,* **8,** 381–396.

Rossow, W. B., and L. C. Garder, 1993a: Cloud detection using satellite measurements of infrared and visible radiances for ISCCP. *J. Climate,* **6,** 2341–2369.

——, and ——, 1993b: Validation of ISCCP cloud detections. *J. Climate,* **6,** 2370–2393.

——, A. W. Walker, and L. C. Garder, 1993: Comparison of ISCCP and other cloud amounts. *J. Climate,* **6,** 2394–2418.

Stohlgren, T. J., T. N. Chase, R. A. Pielke Sr., T. G. F. Kittel, and J. S. Barron, 1998: Evidence that local land use practices influence regional climate, vegetation, and stream flow patterns in adjacent natural areas. *Global Change Biol.,* **4,** 495–504.

Tett, S. F. B., P. A. Stott, M. R. Allen, W. J. Ingram, and J. F. B. Mitchell, 1999: Causes of twentieth-century temperature change near the earth's surface. *Nature,* **399,** 569–572.

Tucker, C. J., J. R. G. Townshend, and T. E. Goff, 1985: African land-cover classification using satellite data. *Science,* **227,** 369–375.

——, I. Y. Fung, C. D. Keeling, and R. H. Gammon, 1986: Relationship between atmospheric CO_2 variations and a satellite-derived vegetation index. *Nature,* **319,** 195–199.

Williams, M., 1989: *Americans and Their Forests: A Historical Geography.* Cambridge University Press, 599 pp.